

*Chapter 1*

## INTRODUCTION

### 1.1 Optical defects and their applications in quantum information technologies

Quantum technologies have been extensively pursued for practical applications which classical system cannot achieve. This includes quantum key distribution (QKD) for unconditionally secure communication [1–3], quantum computers for efficiently simulating complex physical quantum systems [4–6] and quantum sensing with higher sensitivity [7–9]. Quantum technologies take advantage of the quantum mechanical aspects of systems such as the no cloning theorem [10], superposition states and entanglement to surpass the classical limit. Analogous to the term "bit" used for classical information, a unit of quantum information can be denoted as quantum bit, or "qubit". A qubit can be  $|0\rangle$ ,  $|1\rangle$  or any superposition state of the two states [11]:

$$|\psi\rangle = \alpha_0|0\rangle + \alpha_1|1\rangle \quad (1.1)$$

$$|\alpha_0|^2 + |\alpha_1|^2 = 1 \quad (1.2)$$

This is unlike classical bits, which can only be in the 0 or 1 state. Qubits are two-level quantum systems in the Hilbert space spanned by  $|0\rangle$  and  $|1\rangle$  states. Quantum information networks will have an important role in scaling up to globally distributed quantum technologies by interconnecting quantum computers or communication sites [12–14]. Qubits with long coherence time are necessary for quantum information storage. Photons are ideal for transport of quantum information because they can travel a long distance with minimum decoherence [15]. That is why qubit-photon interfacing via bright optical transitions is highly desired. There are three essential requirements for qubits that can be practically used for optical quantum communication [16]:

- (1) There are two long-lived and coherent spin states that are nondegenerate, which corresponds to pure  $|0\rangle$  and  $|1\rangle$  state. (Qubit state longevity)
- (2) There exists optical pumping cycles that can polarize the spin to each pure qubit state. (Optical qubit state initialization)

(3) Luminescence corresponding to each pure qubit state can be differentiated with intensity, wavelength or in other ways. (Optical qubit state readout).

For an example the lowest two states of a spin-1 particle,  $|m_s = -1\rangle$  and  $|m_s = 0\rangle$  can be used as  $|0\rangle$  and  $|1\rangle$  of a qubit [17, 18]. How well this system works compared to an ideal two-level quantum system is characterized by the decoherence induced by coupling to other existing states[19]. A good measure of decoherence for a single qubit is the lifetime of an arbitrary superposition state such as  $(\alpha_0|0\rangle + \alpha_1|1\rangle)/\sqrt{|\alpha_0|^2 + |\alpha_1|^2}$ , denoted by  $T_2$ .

As shown in figure 1.1, a scalable optical quantum network should include the following three components: quantum channels, quantum processors and quantum repeaters [20]. Quantum channels are used to transmit qubits either via free space or via optical fibers. Quantum processors at the end nodes can range from processing simple measurements of qubits for communication to complex qubit manipulation for computing. Because photon loss cannot be avoided, error correction of transmitted quantum information is necessary. Quantum repeaters are inserted at regular intervals in the quantum channels to correct errors accumulated in transmission at long distance.

An initial optical quantum network was demonstrated with trapped atoms in optical resonators [21, 22]. Although the technology for controlling trapped atoms is mature [23], trapping a single atom requires a relatively large and complicated setup and is hard to scale it up due to its volume. On the other hand, solid state system can host many qubits in the crystal within a small volume. Solid state qubits are practical for scaling up due to the potential for compact chip size and easiness of on-chip integration [24, 25]. Many different solid state qubits have been investigated, such as semiconductor quantum dots, defects or impurities in diamond, silicon carbide (SiC), silicon and rare earth ions.

The state of the art QKD demonstration was performed with nitrogen vacancy (NV) centers in diamond. This experiment established entanglement between two NV electron spins separated by 1.3 km confirmed by a loophole-free Bell inequality test [18]. The capability of purifying entangled states was also demonstrated, an important milestone in scaling up the quantum network [26]. However, NV centers suffer from a low fraction of coherent photons emitted into the zero phonon line (ZPL) and spectral diffusion, which hinders the entanglement rate. Also, the nanofabrication procedure for diamond photonic devices is not easy. It is highly possible to create surface charges on the host material during fabrication that increase

spectral diffusion of optical linewidth [27, 28]. The state of the art experimental achievements in NV centers stimulated the search for other candidate qubits in other materials that are closer to ideal qubits with long coherence time and with better optical stability.

It is reasonable to search for color centers in wide bandgap materials similar to diamond, which can have optically active deep level states. It would be beneficial if these materials are common and affordable semiconductors, such as silicon, GaAs, or SiC for future mass production. These materials are also more compatible with existing photonic integrated circuits than diamond. With these ideas in mind, different defects in SiC were recently investigated and found to be attractive as qubits. Among these, divacancies in 4H-SiC have the longest coherence time so far. In the following few sections, I will discuss different types and structure of the host material silicon carbide and divacancies in 4H-SiC in more detail.

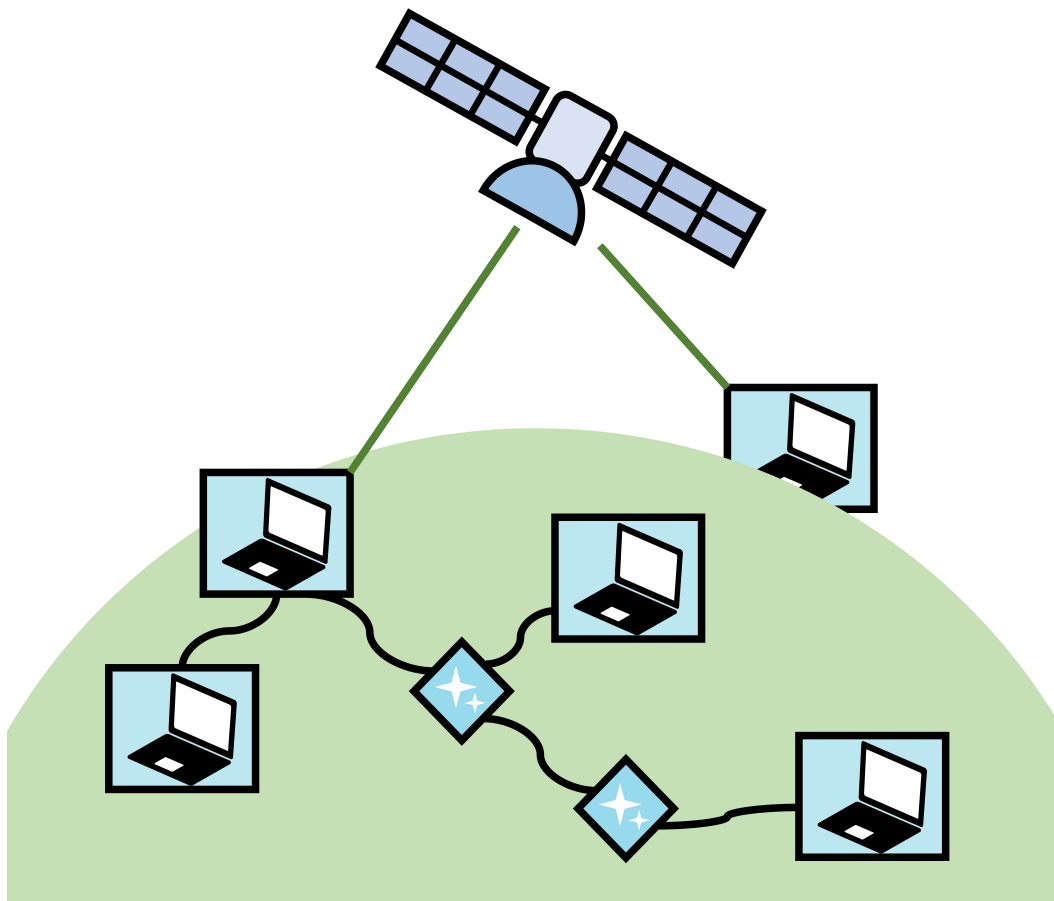


Figure 1.1: An optical quantum network consists of three components: Quantum channels (black or green lines), quantum processors (laptop icons) and quantum repeaters (star icons)

## 1.2 Silicon Carbide (SiC) material background

Silicon carbide (SiC) has been considered as a promising material for power electronics because of its excellent thermal conductivity, high maximum current density, small coefficient of thermal expansion and high melting point. It also has good mechanical properties and is suitable for MEMS devices. These advantages led to the development of wafer mass production and microfabrication in SiC. Although pure SiC has excellent properties, its commercialization was delayed compared to silicon due to poor electric performance caused by defects created during growth and fabrication process. The removal of the defects to unleash the electronic capability of SiC is an ongoing challenge. Some defects and impurities in SiC have been found to emit light at specific wavelength. Photoluminescence spectroscopy can be used to identify different defects and impurities in SiC. The existence of a rich literature about optical identification of these unwanted defects, accelerated the identification of potential qubits.

## 1.3 Polytypes of SiC and 4H-SiC crystal structure

In this section, the crystal structure of SiC is discussed for explaining divacancy photoluminescence in the later section. SiC is known to occur in different crystalline forms. Within those polymorphs, there are more than 150 polytypes [29]. Polytypes have the identical layer structure but differ in stacking sequence in the direction of crystal axis. The smallest periodic component of the SiC crystal structure is shown in figure 1.2. Ideally, 4 silicon atoms and one carbon atom (or vice versa) form a tetrahedron in this structure. If you look at any plane that intersects two silicon-carbon bonds (the 1120 plane and others related by a  $120^\circ$  rotation around c-axis), the structure looks like the right side of figure 1.2. If we set the crystal axis (c-axis) parallel to one bond (c), another in-plane bond (a) forms a  $\sim 109.5^\circ$  angle with this c-axis. In perfect tetrahedra,  $c=a$ . However, the different stacking sequence of SiC layers change the equilibrium of electron structure which results in an elongated (c) bond for hexagonal SiC polytypes [30].

The common commercially used SiC polytypes are 3C, 4H, and 6H-SiC. 3C-SiC has cubic close-packed (fcc) crystal structure and 2H-SiC has hexagonal close-packed (hcp) structure. The stacking of 3C, 2H, 4H and 6H-SiC is shown in figure 1.3. Polytypes are often characterized by hexagonality, the fraction of local hexagonal crystal environment in the entire crystal structure, which is an important parameter influencing physical properties of SiC [31]. Carbon and silicon layers in 4H-SiC stack in ABCB pattern. 4H-SiC has half layers of quasi-hexagonal environment

and 50% hexagonality. Quasi-hexagonal (h) sites and quasi-cubic (k) lattice sites occur when silicon-carbon bilayers alternate between 2H-SiC and 3C-SiC as shown in the left side of figure 1.4. A particular bilayer experiences a different crystal field depending on whether it sees itself in hexagonal or cubic environment, considering the nearest neighbors.

#### 1.4 Divacancies ( $V_C V_{Si}$ ) in SiC as promising qubits

As its name suggests, a single divacancy defect consists of double vacancies at neighbor carbon and silicon sites. Depending on the locations of each vacancy, either h or k site, there are 4 combinations of a divacancy defect shown in the right side of figure 1.4. They are labeled as c-axis divacancies hh (PL1) kk (PL2) and basal (off-axis) divacancies hk (PL3) and kh (PL4). In this thesis, divacancies refer neutrally charged divacancies ( $[V_C V_{Si}]^0$ ).

The quantum potential of divacancy defects was discovered initially by Koehl et al. [32]. This work demonstrated optically detected magnetic resonance (ODMR) and coherent spin polarization of ensemble divacancies. The ground spin state of divacancies can be initialized by a pulse of light and coherently manipulated by microwave pulses. The Ramsey ( $T_2^*$ ) and Hahn echo ( $T_2$ ) microwave pulse sequences were applied to measure spin decoherence characteristics.  $T_2^*$  characterizes the decoherence due to all sources, inhomogeneity of magnetic field within proximity and random spin-spin interactions.  $T_2$  measurements add another pi pulse in the middle of the Ramsey sequence to cancel out the near DC magnetic field inhomogeneity, so  $T_2$  is mainly related to decoherence due to random spin-spin interactions. The ensemble inhomogeneous spin coherence time  $T_2^*$  is  $\sim 1.5 \mu s$  for basal divacancies at 20K and  $\sim 200$  ns for c-axis divacancies at 200K. The ensemble Hahn-echo homogeneous spin coherence time  $T_2$  is  $\sim 200 \mu s$  for basal divacancies at 20K and  $\sim 250 \mu s$  for c-axis divacancies at 200K. Later Christle et al. [33] investigated more on single divacancy properties.  $T_2^*$  of single divacancy is 1 - 5  $\mu s$  at 20 K, similar to ensemble divacancies.  $T_2$  of single PL2 divacancy is 1.2 ms at 20K, which is comparable to that of a NV center [33]. Considering that these results were measured on naturally isotopic 4H-SiC sample (including paramagnetic nuclear spin species  $^{13}C$  1.1%,  $^{29}Si$  4.7%), it is one of the longest Hahn-echo coherence time of an electron spin in solid state crystals [34]. The typical Rabi oscillation period is 0.3  $\mu s$  [33], which suggests there can be  $\sim 4000$  qubit polarization operations before the qubit information is erased by decoherence. This satisfies the practical requirement of fast single qubit operation with high fidelity.

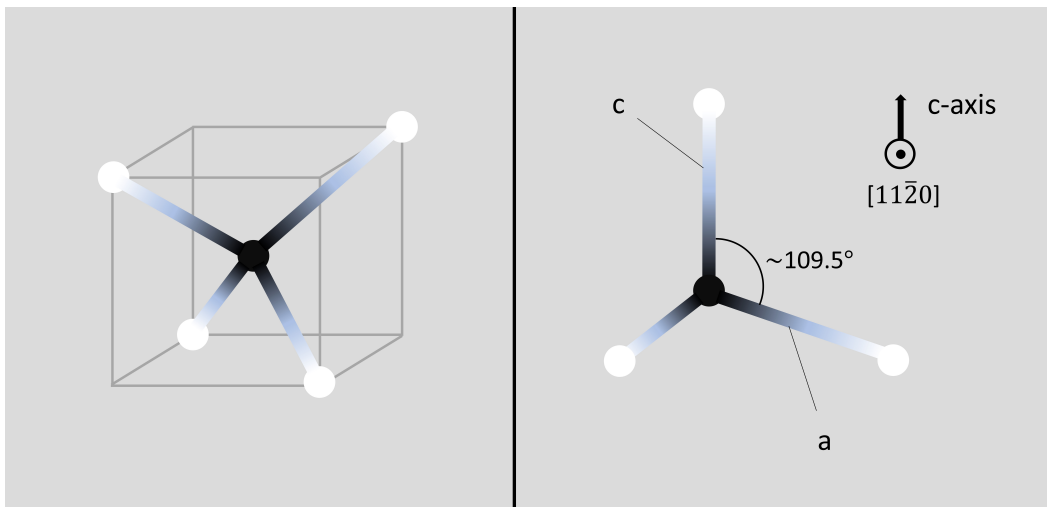


Figure 1.2: Left: the smallest periodic component of the SiC unit cell. The center black sphere shows a Si (C) atom and the white spheres show C (Si) atom. Right: The SiC ideal tetrahedral component viewed in the plane that is parallel to connected straight line connecting two nearest atoms of same kind ( $11\bar{2}0$  plane).

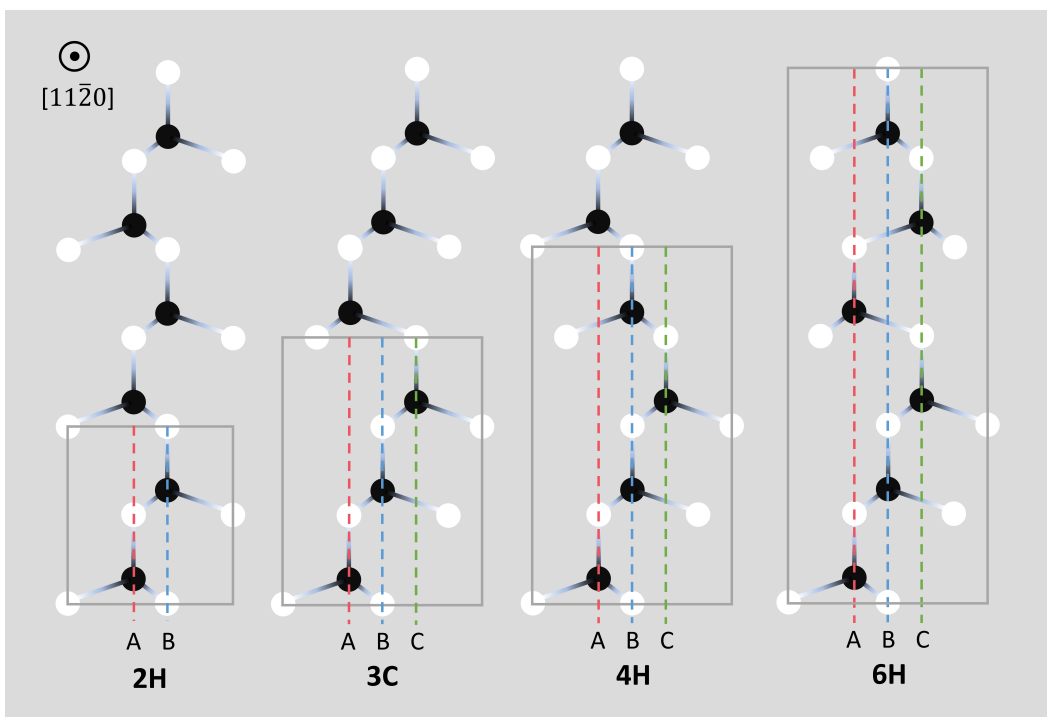


Figure 1.3: 2H, 3C, 4H and 6H-SiC stacking structure viewed in the  $11\bar{2}0$  plane. The gray frame shows the unit cell of each structure.

### 1.5 Coupling optical defects to cavities

Optical quantum networks using solid state qubits require quantum information transmitted by photons to be stored for processing at the end nodes. In free space,

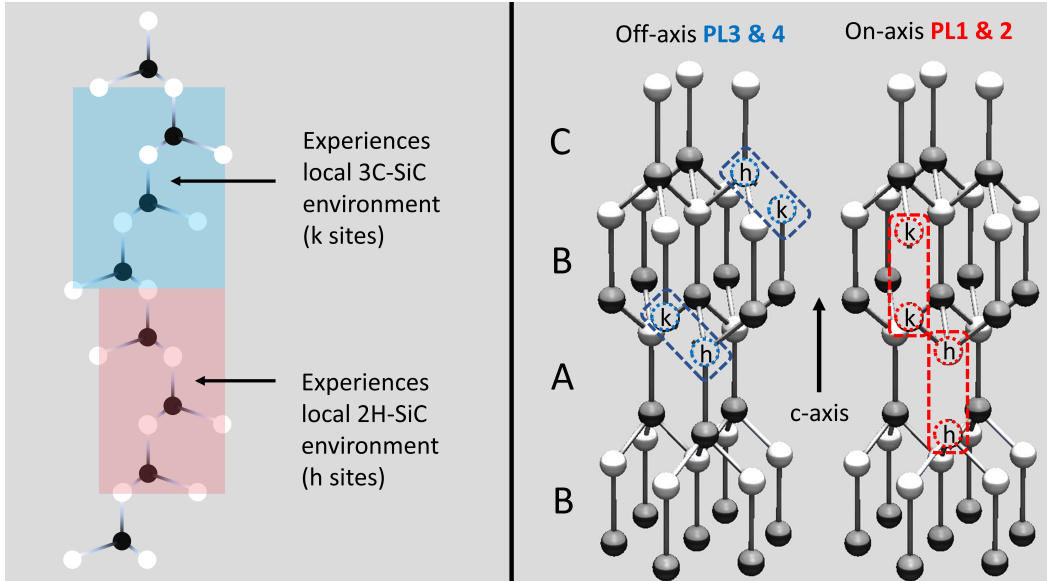


Figure 1.4: Left: Local hexagonal (2H-SiC) or cubic (3C-SiC) environment changes crystal field on atoms in bilayers of 4H-SiC. Right: 3D view of 4H-SiC crystal structure with 4 possible divacancy configuration.

the interaction or absorption cross section between atoms and photons is very small and it is hard to deterministically transfer quantum information between them with time much shorter than the time it can be preserved (atomic coherence time) [35]. Placing optically addressable solid state qubits in an optical cavity enhances the interaction rate between the qubit and the photon because the cavity traps the photon for a longer time and also confines it thus increasing the electric field corresponding to a single photon. This significantly boosts the light-matter interaction and is necessary for deterministic photon-qubit interaction. The cavity-qubit coupling is characterized by the  $g$  parameter which scales as  $\frac{1}{\sqrt{V}}$ , where  $V$  is mode volume of the cavity.

$$V = \frac{\int d^3\mathbf{r} \epsilon(\mathbf{r}) |\mathbf{E}(\mathbf{r})|^2}{\epsilon(\mathbf{r}_{max}) |\mathbf{E}(\mathbf{r}_{max})|^2} \quad (1.3)$$

The system composed of a qubit coupled to a cavity is characterized by the cooperativity parameter. A cooperativity greater than one means that the interaction occurs mainly between the atom and the photon trapped in the cavity before other sources of decoherence become dominant.

There are different types of optical cavities such as Fabry-Perot cavities, microspheres [36], whispering-gallery mode resonators [37], ring resonators [27], photonic crystals [38], etc. Ring resonators are easier to fabricate than photonic crystal

but have large mode volume. Photonic crystals can often achieve less than unit mode volume.

Cavities have the important role to enhance emission of solid state qubits for entanglement generation in QKD application. The state of the art entanglement generation rate using NV centers is 40 Hz [39]. The time to generate quantum entanglement compared to the spin decoherence time indicates how many multiple quantum network links can be maintained. Currently it is on the order of 1 and it needs to be much larger than 1 to reach practical level. Coupling coherent photoluminescence of qubits to optical cavities can greatly reduce its spontaneous emission rate by Purcell enhancement [40], can enhance the emission of a particular transition of interest, and enables better coupling into optical channels like optical fibers, which leads to a significant increase in the entanglement generation rate.

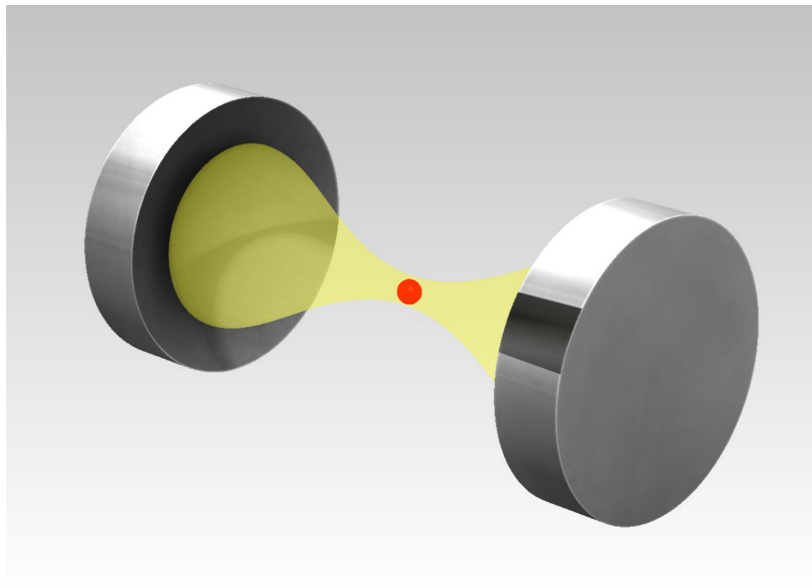


Figure 1.5: Impression of atoms interacting with light in a Fabry-Perot cavity.